



# On the exit-times approach for $\varepsilon$ -entropy and turbulent signals

M. Abel<sup>a</sup>, M. Cencini<sup>a,1</sup>, M. Falcioni<sup>a</sup>, D. Vergni<sup>a</sup>, A. Vulpiani<sup>a,\*</sup>,  
L. Biferale<sup>b</sup>

<sup>a</sup>*Department of Physics and INFN, University of Rome "La Sapienza", p.le Aldo Moro 2,  
I-00185 Roma, Italy*

<sup>b</sup>*Department of Physics and INFN, University of Rome "Tor Vergata", via della Ricerca Scientifica 1,  
I-00133 Roma, Italy*

---

## Abstract

We review a recently proposed approach to the computation of the  $\varepsilon$ -entropy of a given signal based on the exit-time statistics, i.e., one codes the signal by looking at the instants when the fluctuations are larger than a given threshold,  $\varepsilon$ . Moreover, we show how the exit-times statistics, when applied to experimental turbulent data, is able to highlight the intermediate-dissipative-range of turbulent fluctuations. © 2000 Elsevier Science B.V. All rights reserved.

*PACS:* 05.45.-a; 05.45.Tp; 47.27-i

*Keywords:*  $\varepsilon$ -entropy; Dynamical systems; Turbulence

---

## 1. Introduction

The aim of this contribution is twofold. First, we review an approach for the determination of the  $(\varepsilon, \tau)$ -entropy, based on the analysis of exit-times, recently proposed in Ref. [1]. In few words, the idea consists in looking at the information-content of a string of data, without analysing the signal with a constant sampling time,  $\tau$ , but only when the fluctuations are larger than some fixed threshold,  $\varepsilon$ .

Second, we also present a recent application of exit-time analysis to experimental turbulent data [2]. In this latter case, we show that the exit-time events are naturally dominated by laminar fluctuations in the turbulent flows and, therefore, show a

---

\* Corresponding author.

<sup>1</sup> Present address: Max Planck Institut für Physik Komplexer Systeme, Nöthnitzer Str. 38 D01187 Dresden, Germany.

much extended intermediate-dissipative-range than the usual observable based on direct velocity fluctuations.

## 2. Exit-time for $\varepsilon$ -entropy

It is commonplace to look at natural system as a source of information. The natural problem arising from such a point of view is to quantify the degree of complexity of the investigated system (for a nice review see Ref. [3]). The typical questions may range from the aim to distinguish between stochastic or chaotic systems to the more pragmatic goal of determining the degree of complexity (read predictability) at varying the resolution in phase-space and time [4,5].

To address quantitatively and unambiguously (in principle) the first question the proper mathematical tool is the Kolmogorov–Sinai (*KS*) entropy,  $h_{KS}$  [6]. The main idea is very natural: we must look at the information [7] contained in the time sequence as a probe of the underlying dynamics. This is realized by studying the symbolic dynamics obtained by assigning different symbols to different cells of a finite partition of the phase space. The probability distribution of allowed sequences (words) is selected by the dynamical evolution. The average information-gain is defined by comparing sequences of length  $m$  and  $m + 1$ , in the limit of large  $m$ . Letting the length of the words,  $m$ , to infinity and going to infinitely refined partition, one obtains the *KS*-entropy. The *KS*-entropy measures the degree of complexity of the trajectory and corresponds to the rate of information transmission necessary to unambiguously reconstruct the signal.

Unfortunately, only in simple, low-dimensional, dynamical systems such a procedure can be properly carried out with conventional methods [4,5,8,9]. The reason is that for high-dimensional systems the computational resources are not sufficient to cope with the very high resolution and extremely long time series required. Moreover, in many systems, like in turbulence, the existence of non-trivial fluctuations on different time and spatial scales cannot be captured by the *KS*-entropy. This calls for a more general tool to quantify the degree of predictability which depends on the analysed range of scales and frequencies. This was the aim leading Shannon [10] and Kolmogorov [11,12] to introduce the so-called  $\varepsilon$ -entropy, later generalised to the  $(\varepsilon, \tau)$ -entropy [4,8,9]. Conceptually it corresponds to the rate of information transmission necessary to reconstruct a signal with a finite accuracy  $\varepsilon$ , and with a sampling time interval  $\tau$ . The naive  $(\varepsilon, \tau)$ -computation is usually performed by looking at the Shannon entropy of the coarse-grained dynamics on an  $(\varepsilon, \tau)$ -grid in the phase-space and time. However, this method suffers of many computational drawbacks and it is almost useless for many realistic time-series [5]. Another attempt in this direction is the introduction of the finite size Lyapunov exponent [13,14]. Let us just briefly recall the conventional way to calculate the  $(\varepsilon, \tau)$ -entropy for the case of a time-continuous signal  $x(t)$ , recorded during a (long) time interval  $T$ . One defines an  $\varepsilon$ -grid on the phase-space and a  $\tau$ -grid on time. If the motion is bounded, the trajectory visits only a finite number of cells; therefore to each subsequence of length  $n \cdot \tau$  from  $x(t)$  one can associate a word of

length  $n$ , out of a finite alphabet:  $W_t^n(\varepsilon, \tau) = (S_t, S_{t+\tau}, \dots, S_{t+(n-1)\tau})$ , where  $S_t$  labels the cell containing  $x(t)$ . From the probability distribution of the above words one calculates the block entropies  $H_n(\varepsilon, \tau)$ :

$$H_n(\varepsilon, \tau) = - \sum_{\{W^n(\varepsilon, \tau)\}} P(W^n(\varepsilon, \tau)) \ln P(W^n(\varepsilon, \tau)). \tag{1}$$

the  $(\varepsilon, \tau)$ -entropy per unit time,  $h(\varepsilon, \tau)$  is finally defined as

$$h_n(\varepsilon, \tau) = \frac{1}{\tau} [H_{n+1}(\varepsilon, \tau) - H_n(\varepsilon, \tau)], \tag{2}$$

$$h(\varepsilon, \tau) = \lim_{n \rightarrow \infty} h_n(\varepsilon, \tau) = \frac{1}{\tau} \lim_{n \rightarrow \infty} \frac{1}{n} H_n(\varepsilon, \tau), \tag{3}$$

where for practical reasons the dependence on the details of the partition is ignored, while the rigorous definition is given in terms of the infimum over all possible partitions with elements of diameter smaller than  $\varepsilon$  [4]. Note that the above-defined  $(\varepsilon, \tau)$ -entropy is nothing but the Shannon entropy of the sequence of symbols  $(S_t, S_{t+\tau}, \dots)$  associated with the analysed signal. The Kolmogorov–Sinai entropy,  $h_{KS}$ , is obtained by:  $h_{KS} = \lim_{\tau \rightarrow 0} \lim_{\varepsilon \rightarrow 0} h(\varepsilon, \tau)$ . In the case of discrete-time systems, one can define  $h(\varepsilon) \equiv h(\varepsilon, \tau = 1)$ , and  $h_{KS} = \lim_{\varepsilon \rightarrow 0} h(\varepsilon)$ . In usual continuous-time systems the  $\tau$  dependence disappears from  $h(\varepsilon, \tau)$ , so one can still define an  $\varepsilon$ -entropy per unit time  $h(\varepsilon)$ . In particular, also in a pure deterministic flow one can put  $h(\varepsilon) = h(\varepsilon, \tau = 1)$ .

Let us remind that for a genuine deterministic chaotic system one has  $0 < h_{KS} < \infty$  ( $h_{KS} = 0$  for a regular motion), while for a continuous random process  $h_{KS} = \infty$ . Therefore, in order to distinguish between a purely deterministic system and a stochastic system it is necessary to perform the limit  $\varepsilon \rightarrow 0$  in (3). Obviously, from a physical and/or numerical point of view this is impossible. Nevertheless, by looking at the behaviour of the  $(\varepsilon, \tau)$ -entropy at varying  $\varepsilon$  one can have some qualitative and quantitative insights on the chaotic or stochastic nature of the process. For most of the usual stochastic processes one can explicitly give an estimate of the entropy scaling behaviour when  $\varepsilon \rightarrow 0$  [4]. For instance, in the case of a stationary Gaussian process with power spectrum  $S(\omega) \sim \omega^{-2}$  one has [4]

$$h(\varepsilon) \equiv \lim_{\tau \rightarrow 0} h(\varepsilon, \tau) \sim \frac{1}{\varepsilon^2}. \tag{4}$$

Let us now introduce the main point by discussing in detail the difficulties that may arise in measuring the  $\varepsilon$ -entropy for the following non-trivial example of a chaotic-diffusive map [15],  $x_{t+1} = x_t + p \sin 2\pi x_t$ . When  $p > 0.7326\dots$ , one has a diffusive behaviour on large scales, so one expects

$$h(\varepsilon) \simeq \lambda \quad \text{for } \varepsilon < 1, \quad h(\varepsilon) \propto \frac{D}{\varepsilon^2} \quad \text{for } \varepsilon > 1, \tag{5}$$

where  $\lambda$  is the Lyapunov exponent and  $D$  is the diffusion coefficient. The numerical computation of  $h(\varepsilon)$ , using the standard codification, is highly non-trivial already in this simple system. Indeed, behaviour (5) in the diffusive region is roughly obtained by considering the envelope of  $h_n(\varepsilon, \tau)$  evaluated for different values of  $\tau$ ; while looking

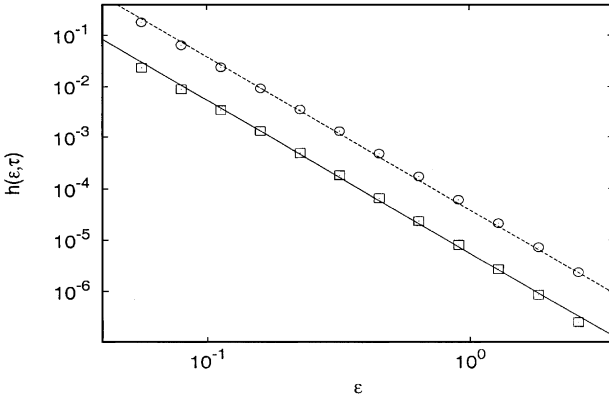


Fig. 1. Numerically computed lower bound (Squares) and upper bound (with  $\tau_e = 0.1(t(\varepsilon))$ ) (Circles) for the  $(\varepsilon, \tau_e)$ -entropy in the case of a self-affine signal with  $\zeta = \frac{1}{3}$  evaluated by using the exit-time approach. The two straight lines show the scaling  $\varepsilon^{-3}$ .

at any single (small) value of  $\tau$  (one would like to put  $\tau = 1$ ) one obtains a rather inconclusive result (see Fig. 1 of Ref. [1]). This is due to the fact that one has to consider very large block lengths  $n$  when computing  $h(\varepsilon, \tau)$ , in order to obtain a good convergence for  $H_n(\varepsilon, \tau) - H_{n-1}(\varepsilon, \tau)$  in (3). Indeed, in the diffusive regime, a simple dimensional argument shows that the characteristic time of the system is  $T_\varepsilon \approx \varepsilon^2/D$ . If we consider, for example,  $\varepsilon = 10$  and typical values of the diffusion coefficient the characteristic time,  $T_\varepsilon$ , is much larger than the elementary sampling time  $\tau = 1$ .

Our approach to calculate  $h(\varepsilon)$  differs from the usual one in the procedure to construct the coding sequence of the signal at a given level of accuracy. Specifically, instead of coding a trajectory according to the symbols  $S_t$ , which label the cells visited by the trajectory at constant time intervals,  $\tau$ , we code it by considering the exit-time,  $t(\varepsilon)$ , and the exit direction (up or down) on an alternating grid of cell size  $\varepsilon$ . We consider the original continuous-time record  $x(t)$  and a reference starting time  $t = t_0$ ; the subsequent exit-time,  $t_1$ , is then defined as the first time necessary to have an absolute variation equal to  $\varepsilon/2$  in  $x(t)$ , i.e.,  $|x(t_0 + t_1) - x(t_0)| \geq \varepsilon/2$ . This is the time the signal takes to exit the cell of size  $\varepsilon$ . Then starting from  $t_1$  we look for the next exit-time  $t_2$ , i.e., the first time such that  $|x(t_0 + t_1 + t_2) - x(t_0 + t_1)| \geq \varepsilon/2$  and so on. Let us note that, with this definition, the coarse-graining grid is not fixed, but it is always centred in the last exit position. In this way we obtain a sequence of exit-times,  $\{t_i(\varepsilon)\}$ , and, moreover, to distinguish the direction of the exit (up or down out of a cell), we introduce the label  $k_i = \pm 1$ , depending whether the signal is exiting above (+1) or below (-1). At the end, the trajectory is univocally coded with the required accuracy, by the sequence  $((t_1, k_1), (t_2, k_2), \dots, (t_M, k_M))$ , where  $M$  is the total number of exit-time events observed during the total time  $T$ . Correspondingly, an “exit-time word” of length  $n$  is a sequence of couples of symbols  $\Omega_i^n(\varepsilon) = ((t_i, k_i), (t_{i+1}, k_{i+1}), \dots, (t_{i+n-1}, k_{i+n-1}))$ . From these words one firstly calculates the block entropies,  $H_n^\Omega(\varepsilon)$ , and then the exit-time  $\varepsilon$ -entropies:  $h^\Omega(\varepsilon) \equiv \lim_{n \rightarrow \infty} H_{n+1}^\Omega(\varepsilon) - H_n^\Omega(\varepsilon)$ . Let us note that  $h^\Omega(\varepsilon)$  is an  $\varepsilon$ -entropy per exit and

that  $M=T/\langle t(\varepsilon) \rangle$ . The exit-time coding is a faithful reconstruction with accuracy  $\varepsilon$  of the original signal. Therefore, the total entropy,  $h^\Omega(\varepsilon)M$ , of the exit-time sequence,  $\Omega^M(\varepsilon)$ , is equal to the total entropy,  $h(\varepsilon)T = h(\varepsilon)N\tau$ , of the standard codification sequence,  $W^N(\varepsilon)$ . Namely, for the  $\varepsilon$ -entropy per unit time, we obtain

$$h(\varepsilon) = Mh^\Omega(\varepsilon)/T = \frac{h^\Omega(\varepsilon)}{\langle t(\varepsilon) \rangle}. \tag{6}$$

Now we are left with the determination of  $h^\Omega(\varepsilon)$ . This implies a discretisation,  $\tau_e$ , of the exit-times. The exit-time entropy  $h^\Omega(\varepsilon)$  becomes an exit-time  $(\varepsilon, \tau_e)$ -entropy,  $h^\Omega(\varepsilon, \tau_e)$ , obtained from the sequence  $\{\eta_i, k_i\}$ , where  $\eta_i$  identifies the exit-time cell containing  $t_i$ . Eq. (6) becomes now

$$h(\varepsilon) = \lim_{\tau_e \rightarrow 0} h^\Omega(\varepsilon, \tau_e)/\langle t(\varepsilon) \rangle \simeq h^\Omega(\varepsilon, \tau_e)/\langle t(\varepsilon) \rangle, \tag{7}$$

the latter relation being valid for small enough  $\tau_e$ . However, in all practical situations there exist a minimum  $\tau_e$  given by the highest acquisition frequency, i.e., the limit  $\tau_e \rightarrow 0$  cannot be reached. The discretisation interval  $\tau_e$  can be thought as the equivalent to the  $\tau$  entering in the usual  $(\varepsilon, \tau)$ -entropy, so that

$$h(\varepsilon, \tau_e) = h^\Omega(\varepsilon, \tau_e)/\langle t(\varepsilon) \rangle. \tag{8}$$

At this point it is important to stress that in most of the cases the leading  $\varepsilon$  contribution to  $h(\varepsilon)$  in (7) is given by the mean exit-time  $\langle t(\varepsilon) \rangle$  and not by  $h^\Omega(\varepsilon, \tau_e)$ . Anyhow, the computation of  $h^\Omega(\varepsilon, \tau_e)$  is compulsory in order to recover a zero entropy for regular (e.g. periodic) signals. It is easy to obtain the following bounds [1]:

$$\frac{h^\Omega(\{k_i\})}{\langle t(\varepsilon) \rangle} \leq h(\varepsilon) \leq \frac{h^\Omega(\{k_i\}) + c(\varepsilon) + \ln(\langle t(\varepsilon) \rangle/\tau_e)}{\langle t(\varepsilon) \rangle}, \tag{9}$$

where  $h^\Omega(\{k_i\})$  is the Shannon entropy of the sequence  $\{k_i\}$  and  $c(\varepsilon) = -\int p(z) \ln p(z) dz$ , and  $p(z)$  is the probability distribution function of the rescaled exit-time  $z(\varepsilon) = t(\varepsilon)/\langle t(\varepsilon) \rangle$ .

The above bounds are rather good, and typically  $\langle t(\varepsilon) \rangle$  shows the same scaling behaviour as  $h(\varepsilon)$ . One could wonder why the exit-time approach is better than the usual one. The reason is simple (and somehow deep): in the exit-time approach it is not necessary to use a very large block size since, at fixed  $\varepsilon$ , the typical time at that scale is automatically given by  $\langle t(\varepsilon) \rangle$ . This fact is particularly clear in the case of Brownian motion. In such a case  $\langle t(\varepsilon) \rangle \propto \varepsilon^2/D$ , where  $D$  is the diffusion coefficient. As previously discussed, the computation of the  $h(\varepsilon)$  with the standard methods implies the use of very large block sizes, of order  $\varepsilon^2/D$ .

Let us now briefly comment the limit  $\varepsilon \rightarrow 0$  for a discrete-time system (e.g. maps). In this limit the exit-time approach coincides with the usual one: we have just to observe that practically the exit-times always coincide with the minimum sampling time and to consider the possibility to have jumps over more than one cell, i.e., the  $k_i$  symbols may take values  $\pm 1, \pm 2, \dots$ . Let us now discuss the  $\varepsilon$ -entropy for a self-affine stochastic signal with Hölder-exponent  $\zeta = \frac{1}{3}$ , i.e.,  $|x(t) - x(t + \Delta t)| \sim (\Delta t)^{1/3}$ . Such a signal can be seen as a stochastic surrogate of a turbulent signal (ignoring intermittency) and

can be constructed in different ways (see Ref. [16] and references therein). A simple dimensional estimate, which is rigorous for Gaussian processes [11,12], tells us that the leading contribution to the  $\varepsilon$ -entropy scaling is given by  $h(\varepsilon) \sim \varepsilon^{-3}$ . To generate the self-affine signal we use a recent algorithm [16], where  $x(t)$  is obtained as product of Langevin processes. In Fig. 1 we show the bounds (9) for  $(\varepsilon, \tau_e)$ -entropy calculated via the exit-times. We observe an extended region of well-defined scaling, which is the same for  $1/\langle t(\varepsilon) \rangle \sim \varepsilon^{-3}$ . The usual approach (not shown) gives a poor estimate for the scaling as the envelope of  $h(\varepsilon, \tau)$  computed for various  $\tau$  (see, for example, Figs. 15–18 in Ref. [4]).

### 3. Exit-times in turbulence

The study of the exit-times statistics have been also demonstrated highlighting for studying some features of turbulent flows. The key point consists in understanding which kind of turbulent events dominate the exit-time statistics, and therefore, what one can learn about turbulence by measuring the exit-times probability distribution.

Let us suppose to have a one-dimensional string of turbulent data (typically the output of an anemometer fixed in some spatial location in the flow). Then one usually investigates velocity fluctuations by studying the so-called structure functions, i.e., moments of velocity increments over a time-delay  $\tau$ :  $S_p(\tau) = \langle\langle [v(t+\tau) - v(t)]^p \rangle\rangle$ , where  $\langle\langle \cdot \rangle\rangle$  indicates the usual time average. It is well known that for time increment corresponding to the inertial range, structure functions develop an anomalous scaling behaviour:  $S_p(\tau) \sim \tau^{\zeta(p)}$ , where  $\zeta(p)$  is a non-linear function, while far inside the dissipative range they show the laminar scaling:  $S_p(\tau) \sim \tau^p$ .

Beside the huge amount of theoretical, experimental and numerical studies devoted to the understanding of velocity fluctuations in the inertial range (see Ref. [17] for a recent overview), only few — mainly theoretical — attempts have focused on the intermediate dissipation range (IDR), introduced in Ref. [18] (see also Refs. [19–22]). By IDR we mean the range of scales,  $\tau \sim \tau_d$ , between the inertial and the dissipative range, where with  $\tau_d$  we denote the dissipative Kolmogorov time.

A non-trivial IDR is connected to the presence of intermittent fluctuations in the inertial range. Namely, anomalous scaling law characterized by the exponents  $\zeta(p)$ , can be explained by assuming that velocity fluctuations in the inertial range are characterized by a spectrum of different local scaling exponents:  $\delta_\tau v = v(t+\tau) - v(t) \sim \tau^h$  with the probability to observe at scale  $\tau$  a value  $h$  given by  $P_\tau(h) \sim \tau^{3-D(h)}$ . This is the multifractal picture of the energy cascade which has been confirmed by many independent experiments [17]. The non-trivial dissipative statistics can be explained by defining the dissipative cut-off as the scale where the local Reynolds number is order of unity

$$\text{Re}(\tau_d) = \frac{\tau_d v_{\tau_d}}{\nu} \sim \text{O}(1). \quad (10)$$

By inverting (10) we obtain a prediction of a fluctuating  $\tau_d$ :  $\tau_d(h) \sim v^{1/(1+h)}$ , where for sake of simplicity we have assumed the large scale velocity,  $U_0$ , and the outer scale,  $L_0$ , both fixed to one.

We review here a recently proposed investigation of exit-time statistics in such a turbulent flows, which has been shown to be able to, to highlight the IDR properties [2]. The main idea is to take a one-dimensional string of turbulent data,  $v(t)$ , and to analyse the statistical properties of the exit times from a set of defined velocity-thresholds. Roughly speaking a kind of *inverse* structure functions [23].

Fluctuations of viscous cut-off are particularly important for all those regions in the fluid where the velocity field is locally smooth, i.e., the local fluctuating Reynolds number is small. In this case, the matching between non-linear and viscous terms happens at scales much larger than the Kolmogorov scale,  $\tau_d \sim v^{3/4}$ . It is natural, therefore, to look for observable which are more sensitive to laminar events. A possible choice is to measure the *exit-time* moments through a set of velocity thresholds. More precisely, given a reference initial time  $t_0$  with velocity  $v(t_0)$ , as in Section 2, we define  $\tau(\delta v)$  as the first time necessary to have an absolute variation equal to  $\delta v$  in the velocity data, i.e.,  $|v(t_0) - v(t_0 + \tau(\delta v))| = \delta v$ . By scanning the whole time series we recover the probability density functions of  $\tau(\delta v)$  at varying  $\delta v$  from the typical large scale values down to the smallest dissipative values. Positive moments of  $\tau(\delta v)$  are dominated by events with a smooth velocity field, i.e., laminar bursts in the turbulent cascade. Let us define the inverse structure functions (Inverse-SF) as

$$\Sigma_p(\delta v) \equiv \langle \langle \tau^p(\delta v) \rangle \rangle, \tag{11}$$

where now one has to consider an average different from the one used to define the  $\varepsilon$ -entropy (see below). According to the multifractal description we suppose that, for velocity thresholds corresponding to inertial range values of the velocity differences,  $\delta_{\tau_d} v \equiv v_m \ll \delta v \ll v_M \equiv \delta_{T_0} v$ , the following dimensional relation is valid:  $\delta_{\tau} v \sim \tau^h \rightarrow \tau(\delta v) \sim \delta v^{1/h}$ . The probability to observe a value  $\tau$  for the exit time is given by inverting the multifractal probability, i.e.,  $P(\tau \sim \delta v^{1/h}) \sim \delta v^{[3-D(h)]/h}$ . Made this ansatz, the prediction for the inverse-SF,  $\Sigma_p(\delta v)$  evaluated for velocity thresholds within the inertial range is:

$$\Sigma_p(\delta v) \sim \int_{h_{\min}}^{h_{\max}} dh \delta v^{[p+3-D(h)]/h} \sim \delta v^{\chi(p)}, \tag{12}$$

where the RHS has been obtained by a saddle point estimate

$$\chi(p) = \min_h \{ [p + 3 - D(h)]/h \}. \tag{13}$$

Let us now consider the IDR properties.

For each  $p$  the saddle point evaluation (13) selects a particular  $h = h_s(p)$ , where the minimum is reached. Let us also remark that from (10) we have an estimate for the minimum value assumed by the velocity in the inertial range given a certain singularity  $h$ :  $v_m(h) = \delta_{\tau_d(h)} v \sim v^{h/(1+h)}$ . Therefore, the smallest velocity value at which the scaling  $\Sigma_p(\delta v) \sim \delta v^{\chi(p)}$  still holds depends on both  $v$  and  $h$ . Namely,  $\delta v_m(p) \sim v^{h_s(p)/(1+h_s(p))}$ .

The most important consequence is that for  $\delta v < \delta v_m(p)$  integral (12) is not any more dominated by the saddle point value but by the maximum  $h$  value still dynamically alive at that velocity difference,  $1/h(\delta v) = -1 - \log(v)/\log(\delta v)$ . This leads for  $\delta v < \delta v_m(p)$  to a pseudo-algebraic law

$$\Sigma_p(\delta v) \sim \delta v^{[p+3-D(h(\delta v))]/h(\delta v)}. \quad (14)$$

The presence of this  $p$ -dependent velocity range, intermediate between the inertial range,  $\Sigma_p(\delta v) \sim \delta v^{\lambda(p)}$ , and the pure dissipative scaling,  $\Sigma_p(\delta v) \sim \delta v^p$ , is the IDR signature. Then, it is easy to show that inverse-SF should display an enlarged IDR. Indeed, for the usual *direct* structure functions the saddle point  $h_s(p)$  value is reached, if  $p > 0$ , for  $h < \frac{1}{3}$ . This pushes the IDR to a range of scales very difficult to observe experimentally [20]. On the other hand, as regards the inverse-SF, the saddle point estimate of positive moments is always reached for  $h_s(p) > \frac{1}{3}$ . This is an indication that we are probing the laminar part of the velocity statistics. Therefore, the presence of the IDR must be felt much earlier in the range of available velocity fluctuations. Indeed, if  $h_s(p) > \frac{1}{3}$ , the typical velocity field at which the IDR shows up is given by  $\delta v_m(p) \sim v^{h_s(p)/(1+h_s(p))}$ , that is much larger than the Kolmogorov value  $\delta v_{r_d} \sim v^{1/4}$ .

Let us make a technical remark. If one wants to compare predictions (12) and (14) with the experimental data, it is necessary to perform the average over the time-statistics in a weighted way. This is due to the fact that by looking at the exit-time statistics we are not sampling the time-series uniformly, i.e., the higher the value of  $\tau(\delta v)$  is, the longer it is detectable in the time series. Let us call  $\tau_1(\delta v), \tau_2(\delta v), \dots, \tau_N(\delta v)$  the string of exit time values obtained by analysing the velocity string data consecutively for a given  $\delta v$ .  $N$  is the number of times for which  $\delta_\tau v$  reaches a given threshold. It is easy to realize [13,14] that the sequential time average of any observable based on exit-time statistics,  $\langle \tau^p(\delta v) \rangle \equiv (1/N) \sum_{i=1}^N \tau_i^p$ , is connected to the uniformly-in-time multifractal average,  $\langle\langle (\cdot) \rangle\rangle \equiv \int dh(\cdot)$ , by the relation

$$\langle\langle \tau^p(\delta v) \rangle\rangle = \sum_{i=1}^N \tau_i^p \frac{\tau_i}{\sum_{j=1}^N \tau_j} = \frac{\langle \tau^{p+1} \rangle}{\langle \tau \rangle}, \quad (15)$$

where  $\tau_i / \sum_{j=1}^N \tau_j$  takes into account the non-uniformity in time. Incidentally, we observe that according to Eq. (15), the average exit-time used in the definition of the  $\varepsilon$ -entropy (6) corresponds to  $\Sigma_{-1}(\varepsilon)$  which is proportional to  $\varepsilon^{-3}$ , so that even considering the intermittency correction for one-dimensional turbulent signal one has  $h(\varepsilon) \sim \varepsilon^{-3}$ .

Let us now go back to the typical behaviour showed by high-Reynolds inverse-SF. As one can see in Fig. 1 of Ref. [2], the inverse-SF have a very poor scaling behaviour also at high Reynolds. We interpret this as a clear evidence of IDR's contamination into the whole range of available velocity values for the inverse-SF cases.

In order to better understand the scaling properties of  $\Sigma_p(\delta v)$  we also investigated a synthetic multi-affine field obtained by combining successive multiplications of Langevin dynamics [16]. The advantage of using a synthetic field is that one can control analytically the scaling properties of direct structure functions in order to have



the same scaling laws observed in experimental data. An IDR can be introduced in the synthetic signals by smoothing the original dynamics on a moving time-window of size  $\delta T$ . Imposing a smoothing time-window is equivalent to fixing the Reynolds numbers,  $Re \sim \delta T^{-4/3}$ . The purpose to introduce this stochastic multi-affine field is twofold. First we want to reach high Reynolds numbers enough to test the inverse-multifractal formula (13). Second, we want to test that the very extended IDR observed in the experimental data is also observed in this stochastic field. This would support the claim that the experimental result is the evidence of an extended IDR.

As for the first point, it was shown in Ref. [2] that the inverse-SF,  $\Sigma_1(\delta v)$ , measured in the multiaffine synthetic signal at high-Reynolds numbers are in perfect agreement with prediction (13). The same agreement also holds for higher moments, see Table 1 of Ref. [2]. Let us now go back to the most interesting question about the statistical properties of the IDR. In order to study this question we have smoothed the stochastic field,  $v(t)$ , by performing a running-time average over a time-window,  $\delta T$ . Then we compare inverse-SF scaling properties at varying Reynolds numbers, i.e., for different dissipative cut-off:  $Re \sim \delta T^{-4/3}$ .

Expression (14) predicts the possibility to obtain a data collapse of all curves with different Reynolds numbers by rescaling the inverse-SF as follows [18,19]:

$$-\frac{\ln(\Sigma_p(\delta v))}{\ln(\delta T/\delta T_0)} \text{ vs. } -\frac{\ln(\delta v/U)}{\ln(\delta T/\delta T_0)}, \tag{16}$$

where  $U$  and  $\delta T_0$  are adjustable dimensional parameters. Within the same experimental (or synthetic) set up they are Reynolds number independent (i.e.,  $\delta T$  independent).

The rationale for rescale (16) stems from the observation that, in the IDR,  $h_s(p)$  is a function of  $\ln(\delta v)/\ln(v)$  only. Therefore, identifying  $Re \propto v^{-1}$ , relation (16) directly follows from (14). This rescaling was originally proposed as a possible test of IDR for direct structure functions in [18] but, as already discussed above, for the latter observable it is very difficult to detect any IDR due to the extremely small scales involved [20].

Fig. 2 shows the rescaling (16) of the inverse-SF,  $\Sigma_1(\delta v)$ , for the synthetic field at different Reynolds numbers and for the experimental signals. As it is possible to see, the data-collapse is very good for both the synthetic and experimental signal. This is a clear evidence that the poor scaling range observed for the experimental signal can be explained as the signature of the IDR. The same behaviour holds for higher moments (not shown).

It is interesting to remark that for a self-affine signal (i.e., a unique possible value for  $h$  and  $D(h = \frac{1}{3}) = 3$ ), the IDR is highly reduced and the inverse-SF, scaling trivially as  $\Sigma_p(\delta v) \sim (\delta v)^{3p}$ , do not bring any new information.

Let us summarize the results here discussed. First, by defining the exit-time moments,  $\Sigma_p(\delta v)$ , we argued that they must be dominated by the laminar part of the energy cascade. This implies that they depend only on the part of  $D(h)$  which falls to the right of its maximum, i.e.,  $h > \frac{1}{3}$ . These  $h$ 's values are not testable by the

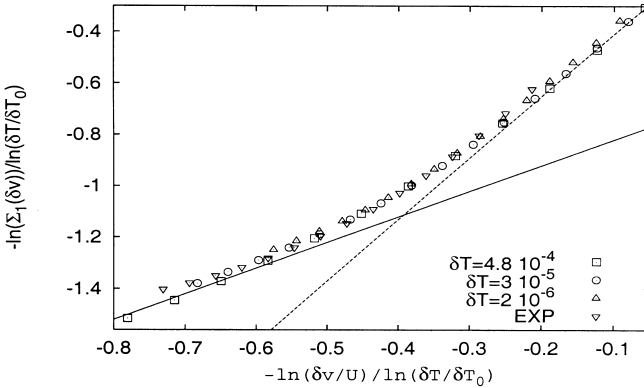


Fig. 2. Data collapse of the inverse-SF,  $\Sigma_1(\delta v)$ , obtained by rescaling (16) for the smoothed synthetic signals (with time windows:  $\delta T = 4.8 \times 10^{-4}$ ,  $3 \times 10^{-5}$ ,  $2 \times 10^{-6}$ ) and the experimental data (EXP). The two straight lines have the dissipative (solid line) and the inertial range (dashed) slope.

direct structure functions. Inverse-SF are the natural tool to test any model concerning velocity fluctuations less singular than the Kolmogorov value  $\delta v \sim \tau^{1/3}$ .

Second, by analysing high-Reynolds data and synthetic fields, we have proved that the extension of the IDR for  $\Sigma_p(\delta v)$  is magnified. Moreover, the rescaling (16) based on the assumption (10) gives a good data collapse of all curves for different Reynolds numbers. This is a clear evidence of the IDR.

#### 4. Conclusions

In conclusion, we have reviewed some recent investigations on the exit-time approach to calculate  $\varepsilon$ -entropy in stochastic and deterministic systems [1] and on the exit-time approach to highlight the IDR of turbulent data [2]. In both cases we have shown how to look at ‘inverse’ statistical estimator can improve our understanding of the underlying dynamics, both from the entropic-point of view as for the case of the  $\varepsilon$ -entropy calculation or for the role played by viscous dissipation at not too small scales as for the case of the intermediate-dissipative-range.

#### Acknowledgements

We acknowledge useful discussions with G. Boffetta, A. Celani, U. Frisch, M.H. Jensen, and M. Vergassola. This work has been partially supported by INFM (PRA-TURBO) and by the European Network *Intermittency in Turbulent Systems* (contract number FMRX-CT98-0175). M.A. is supported by the European Network *Intermittency in Turbulent Systems*.

## References

- [1] M. Abel, L. Biferale, M. Cencini, M. Falcioni, D. Vergni, A. Vulpiani, An exit-time approach to  $\varepsilon$ -entropy, *chao-dyn*/9912007.
- [2] L. Biferale, M. Cencini, D. Vergni, A. Vulpiani, *Phys. Rev. E* 60 (1999) R6295.
- [3] R. Badii, A. Politi, *Complexity, Hierarchical Structures and Scaling in Physics*, Cambridge University Press, Cambridge, 1997.
- [4] P. Gaspard, X.-J. Wang, *Phys. Rep.* 235 (1993) 291.
- [5] H. Kantz, T. Schreiber, *Nonlinear Time Series Analysis*, Cambridge University Press, Cambridge, 1997.
- [6] A.N. Kolmogorov, *Dokl. Akad. Nauk SSSR* 119 (1958) 861.
- [7] C.E. Shannon, *Bell Systems Techn. J.* 27 (1948) 379, 623.
- [8] P. Grassberger, I. Procaccia, *Phys. Rev. Lett.* 50 (1983) 346.
- [9] A. Cohen, I. Procaccia, *Phys. Rev. A* 31 (1985) 1872.
- [10] C.E. Shannon, W. Weaver, *The Mathematical Theory of Communication*, University of Illinois Press, Urbana, Illinois, 1949.
- [11] A.N. Kolmogorov, *IRE Trans. Inform. Theory* 1 (1956) 102.
- [12] I.M. Gelfand, A.N. Kolmogorov, A.M. Yaglom, in: A.N. Shiryeyev (Ed.), *Selected Works of A.N. Kolmogorov, Vol. III* (1958), Kluwer Academic Publishing, Dordrecht, 1993, p. 33.
- [13] E. Aurell, G. Boffetta, A. Crisanti, G. Paladin, A. Vulpiani, *Phys. Rev. Lett.* 77 (1996) 1262.
- [14] E. Aurell, G. Boffetta, A. Crisanti, G. Paladin, A. Vulpiani, *J. Phys. A* 30 (1997) 1.
- [15] M. Schell, S. Fraser, R. Kapral, *Phys. Rev. A* 26 (1982) 504.
- [16] L. Biferale, G. Boffetta, A. Celani, A. Crisanti, A. Vulpiani, *Phys. Rev. E* 57 (1998) R6261.
- [17] U. Frisch, *Turbulence, The legacy of A.N. Kolmogorov*, Cambridge University Press, Cambridge, 1995.
- [18] U. Frisch, M. Vergassola, *Europhys. Lett.* 14 (1991) 439.
- [19] M.H. Jensen, G. Paladin, A. Vulpiani, *Phys. Rev. Lett.* 67 (1991) 208.
- [20] Y. Gagne, B. Castaing, *C. R. Acad. Sci. Paris* 312 (1991) 441.
- [21] R. Benzi, L. Biferale, S. Ciliberto, M.V. Struglia, R. Tripiccone, *Physica D* 96 (1996) 162.
- [22] V.S. L'vov, I. Procaccia, *Phys. Rev. E* 54 (1996) 6268.
- [23] M.H. Jensen, *Phys. Rev. Lett.* 83 (1999) 76.